






## Research Article

# Silver Nanoparticles Based on *Annona muricata* Peel Reduce Cell Viability in Medulloblastoma and Neuroblastoma Cell Lines

**Eduardo Lira-Díaz** <sup>1,2</sup>, **Ricardo Cruz-Márquez**,<sup>3</sup> **María Guadalupe González-Pedroza** <sup>3</sup>,  
**Oscar Gonzalez-Perez** <sup>4</sup>, **Raúl Alberto Morales-Luckie** <sup>1</sup>,  
**and Juan José Acevedo-Fernández** <sup>2</sup>

<sup>1</sup>Laboratorio de Nanomateriales, Centro Conjunto de Investigación en Química Sustentable, UAEMex-UNAM, Carretera Km. 14.5, Unidad San Cayetano, Toluca-Atlacomulco, Toluca de Lerdo 50200, Estado de México, Mexico

<sup>2</sup>Laboratorio de Biología de Células Troncales, Facultad de Medicina, UAEM, Leñeros S/N, Los Volcanes, Cuernavaca 62350, Morelos, Mexico

<sup>3</sup>Departamento de Biotecnología, Facultad de Ciencias, UAEMex, Carretera Toluca-Ixtlahuaca Km. 15.5, Piedras Blancas, Toluca de Lerdo 50200, Estado de Mexico, Mexico

<sup>4</sup>Laboratorio de Neurociencias, Facultad de Psicología, Universidad de Colima, Avenida Universidad 333, Las Víboras, Colima City 28040, Colima, Mexico

Correspondence should be addressed to Juan José Acevedo-Fernández; [juan.acevedo@uaem.mx](mailto:juan.acevedo@uaem.mx)

Received 22 June 2024; Accepted 27 August 2024

Academic Editor: Luis Jesús Villarreal-Gómez

Copyright © 2024 Eduardo Lira-Díaz et al. This is an open access article distributed under the Creative Commons Attribution License, which permits unrestricted use, distribution, and reproduction in any medium, provided the original work is properly cited.

Silver nanoparticles (AgNPs) can be obtained from plants and other organisms through green synthesis methods, considered eco-friendly and highly biocompatible. In this way, using plants with antitumor bioactive compounds increases cytotoxicity against tumor cells, acting in synergy between plant bioactive compounds (covering the nanoparticle) and AgNPs by itself. Acetogenins are the signature bioactive compounds present in *Annona muricata* (soursop) that induce tumor cell death by blocking respiratory complex 1 of the electron transport chain of the mitochondria, which is overexpressed in high-grade tumors such as medulloblastoma, a high-grade tumor of embryonic origin that affects the pediatric population. In this study, we evaluated the effects of AgNPs derived from an aqueous extract of soursop peel on neuroblastoma (CHP-212) and medulloblastoma (Daoy and D341 Med) cell lines. Additionally, we evaluated the viability of fibroblasts (HDFn) and macrophages (RAW 264.7) to observe biosafety in nontumor cells. Our results showed that AgNPs in soursop peel reduced the viability of CHP-212, Daoy, and D341 Med cell lines, in contrast to the fibroblast cell line. Thus, AgNPs derived from the aqueous extract of soursop peel may serve as a promising therapeutic tool for treating brain tumors.

## 1. Introduction

AgNPs (1–100 nm) are structures of nanometric scale that have emerged as a new method for treating several diseases [1]. AgNPs can be obtained with relatively easy synthesis methods and present high biocompatibility and functionalization (attachment) to molecules with clinical relevance; thus, AgNPs have been widely investigated as a therapeutic approach in cancer research [2, 3]. Green/biological synthesis of AgNPs from plants with bioactive compounds that have cytotoxic effects on tumor cells could represent advantages over

chemically synthesized nanoparticles by creating synergistic effects conferred by the antitumor bioactive compounds and the nanoparticles. *Annona muricata* is extensively cultivated in tropical and subtropical areas, such as North and South America, the West Indies, Africa, the Pacific Islands, and Southeast Asia for the food industry [4, 5]. Despite its dietary importance, soursop is known to possess acetogenins, anti-tumor bioactive compounds present in the leaves, roots, bark, and fruit, targeting multiple molecular pathways involved in crucial functions of the pancreatic, cervical, colon, lung, breast, and prostate tumor among others [6–11].

Recently, it has been demonstrated that AgNPs synthesized from *A. muricata* leaves and fruit peel reduced the viability of colon, breast, and melanoma cell lines, even in comparison to the aqueous extracts alone [2]. In this study, we investigated AgNPs synthesized from soursop peel in medulloblastoma and neuroblastoma cell lines (grades 4 and 2–4, respectively; World Health Organization (WHO) [12–14]) and tested nontumor cell lines from macrophages and fibroblasts. Cancerous cells display a wide range of differences in cellular processes between tumor types. Both medulloblastoma and neuroblastoma are in the embryonal tumor classification [15], but as mentioned above, they differ in grade severity. The grade of severity is crucial when treatment is determined; since grade 4 tumors are more vascularized and exacerbate the proliferation activity of aberrant cells [16, 17], the efficacy of the AgNPs is supposed to be different. Here, we demonstrated that AgNPs are cytotoxic to neuroblastoma and medulloblastoma cell lines regarding cell viability. This suggests that AgNPs derived from the aqueous extract of soursop peel inhibit the proliferation of high-grade brain tumors.

## 2. Materials and Methods

**2.1. Biosynthesis of Silver Nanoparticles.** The fruits of *A. muricata* were collected from the municipality of Xochitepec (18°46'52" N, 99°12'02" W) in the state of Morelos, between June and July when the maturity of the fruit is reached. The fruit peel was processed as previously described [2]. To obtain *A. muricata* peel extract, 1 g of peel powder was added to 100 mL of sterile distilled water and heated to 100°C for 5 min. Then, the extract was filtered with a filter paper (Whatman No. 1), and a second filtration was carried out with 0.22  $\mu\text{m}$  syringe filters.

To synthesize the AgNPs, a silver nitrate solution ( $1 \times 10^{-2}$  M; Sigma, Cat. 209139) was added to the extract in a relation 1:1, and the mixture was placed in a well-illuminated section of the lab, exposed to direct sunlight for 5–7 minutes at room temperature. Finally, the AgNPs' solution was removed from the light and left at room temperature for six hours to allow the AgNPs to grow. The extract and AgNPs were synthesized using a previously reported method [2]. To prepare the AgNP solution in a cell culture medium, the aqueous solution of AgNPs was centrifuged at 6,000 rpm at 23–24°C for 20 minutes and resuspended in a free serum culture medium. To dissolve AgNPs' aggregates, the solution was exposed to sonication for 1–2 seconds. The extract and AgNPs were synthesized on the previous day of the experiment, and the solution of AgNPs in the cell culture medium was obtained on the same day. The cell culture medium depended on the cultured cell line, DMEM/F-12 and DMEM HG. From now on, AgNPs in water (aqueous extract) will be called AgNPs-W and AgNP-M for the AgNPs in the cell culture medium.

**2.2. AgNPs Characterization.** To determine whether AgNPs were present in water and medium, we analyzed both solutions of AgNPs using ultraviolet visible (UV/Vis)

spectroscopy equipment (Varian Cary 5000 UV-Vis-NIR, Agilent Technologies). All samples were analyzed in the 200–800-nm absorption range. Fourier-transform infrared spectrometry (FTIR; Bruker Tensor, Model 27) was used to characterize the functional groups of the molecules that sheathed the AgNPs in both solutions. The equipment was operated under standard conditions (transmittance mode, from 600 to 4,000  $\text{cm}^{-1}$ ). To characterize the size and morphology of the AgNPs in both solutions, we used transmission electron microscopy (TEM) (JEOL-2100 200 kV with LaB<sub>6</sub> filament) and AgNPs were examined and measured with ImageJ software version 1.52p (NIH) as previously described. AgNP characterization was performed according to a previously described protocol [2].

**2.3. Cell Lines and Cell Culture Conditions.** Human fibroblast cell lines (HDFn; ATCC PCS-201-010), neuroblastoma (CHP-212; ATCC CRL-2273), medulloblastoma (Daoy; ATCC HTB-186 and D341 Med; ATCC HTB-187), and mouse macrophages (RAW 264.7; ATCC TIB-71) were used. Fibroblasts, neuroblastoma, and medulloblastoma cell lines were cultured in the DMEM/F12 medium (Dulbecco's modified Eagle's Medium F-12; Gibco, cat. 12500) supplemented with 10% fetal bovine serum (FBS; Biowest, cat. S1650), 20% FBS for D341 Med, and 1% antibiotic-antimycotic solution (Gibco, cat. 15240062), and 2 mM glutamine (Gibco, cat. 25030081), and 1% sodium pyruvate (Gibco, cat. 11360070), while macrophages were cultured in high-glucose DMEM (Dulbecco's Modified Eagle Medium HG; Gibco, cat. 12100046) supplemented with 6% FBS, 1% antibiotic-antimycotic, 2 mM glutamine, and 1% non-essential amino acids (Gibco, cat. 11140050). All the cells were maintained under standard culture conditions at 37°C and 5% CO<sub>2</sub>.

**2.4. MTT Assay for Cell Viability.** To determine cell viability, 3-(4,5-dimethylthiazol-2-yl)-2,5-diphenyltetrazolium bromide (MTT) assay (Biomatik, cat. A3338) was performed and 5,000 cells of each cell line were plated in each well of a 96-well plate and allowed to attach to the surface for 24 h. The peel extract was analyzed at 2,000, 1,000, 500, 250, 125, and 62.5  $\mu\text{g}/\text{mL}$  and the AgNP solutions at 100, 50, 25, 12.5, 6.25, and 3.12  $\mu\text{g}/\text{mL}$  for 72 h. After incubation, the cells were rinsed with PBS and a fresh medium was added. The cells were incubated for 4 h with 10  $\mu\text{L}$  of MTT (5 mg/mL in PBS). Then, 100  $\mu\text{L}$  per well of DMSO (Sigma, cat. 472301) was added, and the absorbance was read at 570 nm. Three independent experiments were performed in triplicates.

**2.5. Statistical Analysis.** For the statistical analysis obtained in the MTT assay, we performed a multivariate parametric one-way ANOVA followed by a *post-hoc* Tukey HSD test to detect statistical differences between the groups. Column bars show the data. Data are expressed as the mean  $\pm$  standard deviation (SD). The  $p \leq 0.05$  value was selected to establish statistically significant differences. IBM SPSS Statistics for Windows, version 21 (IBM Corp., Armonk, N.Y.,

USA) was used to analyze multiple correlations between the groups. Graphs were generated using GraphPad Prism for Windows, version 8 (GraphPad Software Inc., San Diego, CA, USA).

### 3. Results

**3.1. AgNPs Synthesis and UV/Vis Characterization.** As mentioned above, in an attempt to use a safe vehicle solution for nontumor cells, we fixed the water for the cell culture medium, DMEM HG for macrophages, and DMEM/F12. In the UV/Vis analysis, the AgNPs in water showed an emission peak at 435 nm, whereas the AgNPs resuspended in DMEM HG and DMEM/F12 reached plasmon resonances of 440 nm and 440 nm, respectively (Figure 1).

**3.2. Structural and Morphological Characterization of AgNPs.** To corroborate the spheroid morphology, we performed a TEM analysis. We observed spheroid morphology in both solutions, AgNPs in water and cell culture medium (Figures 2(a)(A) and 2(b)(A)). Moreover, we determined a mean size of AgNPs in water of  $14.86 \pm 5.29$  nm, and that of the AgNPs in the cell culture medium was  $17.15 \pm 7.25$  nm in diameter (Figures 2(a)(C) and 2(b)(C)). The interplanar distance in both AgNPs solutions was  $2.36 \text{ \AA}$  (Figures 2(a)(B) and 2(b)(B)), indicating, in both cases, that AgNPs have crystalline structures that correspond to the family of crystalline planes (200), according to the 00-004-0783 of the Joint Committee on Powder Diffraction Standards (JCPDS).

**3.3. FTIR Analysis of AgNPs.** The FTIR spectrum (Figure 3) shows a characteristic absorption band at  $1730 \text{ cm}^{-1}$  (of the extract and the AgNPs) characteristic of a conjugated C=O group, suggesting the presence of  $\gamma$ -lactone- $\alpha$ ,  $\beta$ -unsaturated that is associated with the vast majority of acetogenins; additionally, a shift of these bands is observed in the AgNPs in cell culture medium samples located at  $1662 \text{ cm}^{-1}$ .

**3.4. AgNPs Decrease the Cell Viability of Medulloblastoma (Daoy and D341 Med) and Neuroblastoma (CHP-212) Cell Lines.** As mentioned above, AgNPs obtained from biosynthesis decreased the viability of tumor cells. After 72 hours of incubation with AgNPs, we observed a reduction in the viability of Daoy cells in both groups with AgNPs compared to the extract group at  $100 \mu\text{g/ml}$  (extract:  $37.26 \pm 1.91\%$  vs. AgNP-W:  $21.78 \pm 1.31\%$ ,  $p \leq 0.001^{***}$ ; vs. AgNP-M:  $32.18 \pm 2.23\%$ ,  $p \leq 0.035^*$ ); interestingly, we also found differences between both AgNPs groups, being the AgNPs-W more effective than the AgNPs-M ( $p \leq 0.001^{**}$ ). At  $50 \mu\text{g/ml}$ , we found that AgNPs show a reduced cell viability in comparison to the extract group (Extract:  $77.84 \pm 11.91\%$  vs. AgNP-W:  $49.09 \pm 5.39\%$ ,  $p \leq 0.013^*$ ; vs. AgNP-M:  $51.84 \pm 6.48\%$ ,  $p \leq 0.021^*$ ), and no differences were detected between AgNPs groups ( $p \leq 0.916$ ). No statistically significant differences were observed for other concentrations (Figure 4(a), supplementary Table 1). When we compare to the control positive group (Eto: etoposide),

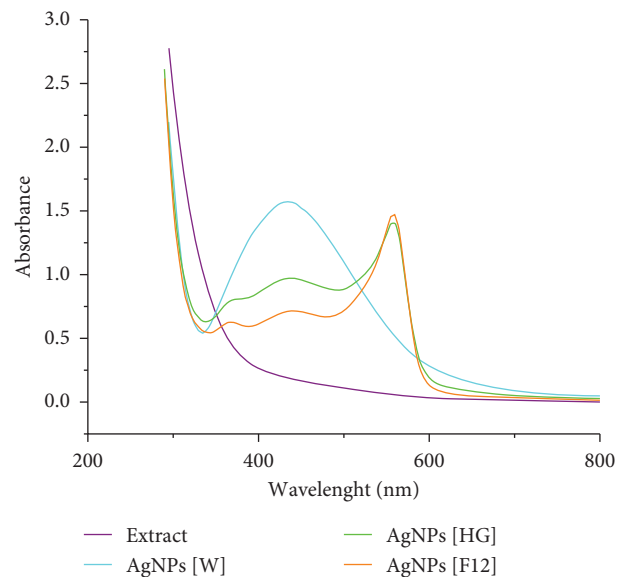


FIGURE 1: Optical characterization of AgNPs. UV/Vis spectra for extract (purple), AgNPs in water-extract (AgNPs [W], light blue), AgNPs in the HG cell culture medium (AgNPs [HG], green), and AgNPs in the F12 cell culture medium (AgNPs [F12], orange).

differences were observed in the three evaluated groups vs. Eto ( $0.5 \text{ mg/ml}$ ) (Figure 4(a), supplementary table 2), Eto:  $47.92 \pm 5.73$  vs. extract, AgNPs-W and AgNPs-M ( $p \leq 0.001^{***}$ ,  $0.001^{****}$ ,  $0.001^{****}$ , respectively). At  $50 \mu\text{g/ml}$ , the AgNPs groups display a similar effect to the Eto group (AgNPs-W:  $p \leq 0.994$ ; AgNPs-M:  $p \leq 0.851$ ); conversely, the extract group loses its toxic effect vs Eto ( $p \leq 0.002^{**}$ ).

We also evaluated cell viability in the D341 Med medulloblastoma cell line, another subtype of medulloblastoma. D341 Med cells in the AgNP-M and AgNPs-W groups decrease their viability compared to the extract group at  $100 \mu\text{g/ml}$  (extract:  $61.02 \pm 7.67\%$  vs. AgNP-W:  $47.37 \pm 2.48$ ,  $p \leq 0.028^*$ ; vs. AgNPs-M:  $46.95 \pm 1.22\%$ ,  $p \leq 0.024^*$ ). A similar pattern was observed at  $50 \mu\text{g/ml}$  (extract:  $79.21 \pm 11.71\%$  vs. AgNP-W:  $52.92 \pm 4.13\%$ ,  $p \leq 0.014^*$ ; vs. AgNPs-M:  $51.54 \pm 5.08\%$ ,  $p \leq 0.011^*$ ). No statistical significances were observed in the other concentrations (Figure 4(b), Supplementary table 3). As in the Daoy cell line, here, we compare to its positive control group, cyclophosphamide (Cyclo) [ $1.5 \text{ mg/ml}$ ]; the analysis shows no differences at  $100 \mu\text{g/ml}$  in any comparison. However, there is an upward trend in the extract group vs Cyclo, suggesting a poor effect of the extract (extract:  $61.02 \pm 7.67\%$  vs. Cyclo:  $50.22 \pm 4.34$ ,  $p \leq 0.051$ ). This effect is pronounced at  $50$  and  $25 \mu\text{g/ml}$ , where differences between extract and Cyclo are evident ( $50 \mu\text{g/ml}$ ,  $p \leq 0.002^{**}$ ;  $25 \mu\text{g/ml}$ ,  $p \leq 0.008^{**}$ ). Meanwhile, no differences were observed between the AgNPs groups vs Cyclo:  $50 \mu\text{g/ml}$ ,  $p \leq 0.934$  and  $0.990$ ;  $25 \mu\text{g/ml}$ ,  $p \leq 0.343$  and  $0.258$ , AgNPs-W and -M, respectively. Figure 4(b) and supplementary table 4).

On the other hand, to evaluate the cell viability in a grade 2–4 tumor cell line, we expose neuroblastoma cells (CHP-212) to AgNPs. Surprisingly, we only found differences at

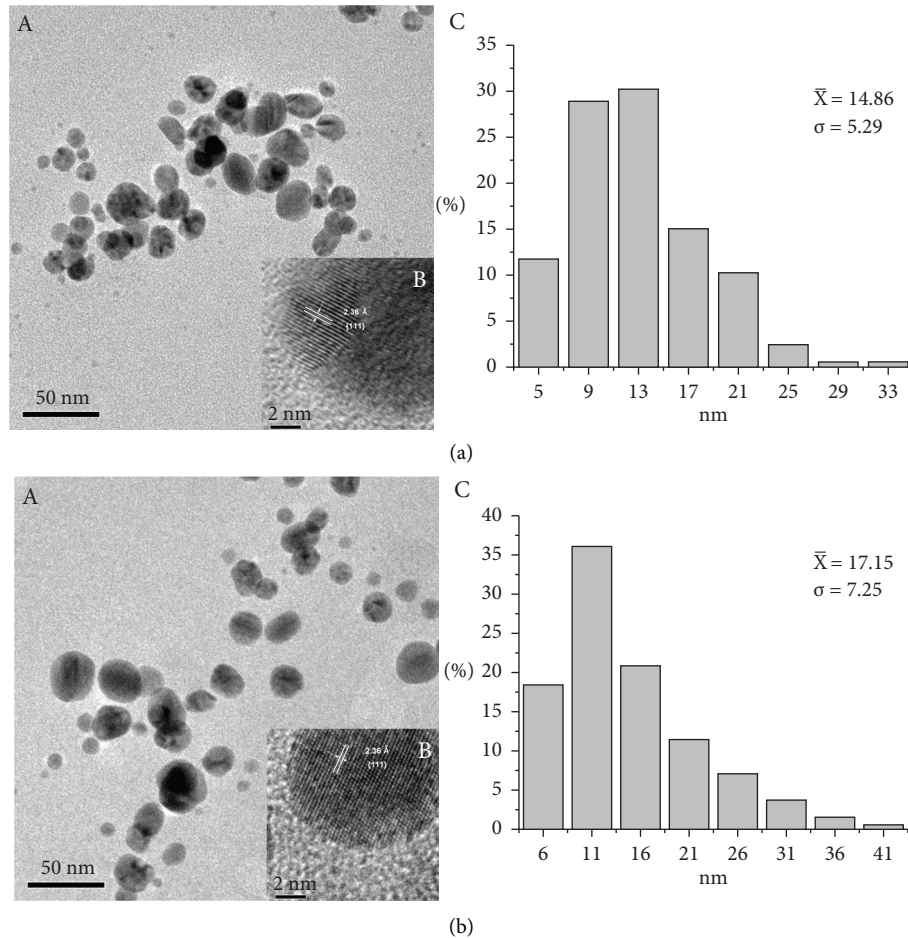


FIGURE 2: Morphological and structural characterization. (a) (A) Spheroid nanoparticles in the water extract with an interplanar distance of 2.36 Å (Amperes) (B) and a mean size of  $14.86 \pm 5.29$  nm of diameter (C). (b) (A) Spheroid nanoparticles with an interplanar distance of 2.36 Å (B) and a mean size of  $17.15 \pm 7.25$  nm of diameter (C). The interplanar distances corroborate that AgNPs are composed of silver. Scale bars = 50 nm (aA and bA) and 2 nm for inserts (aB and bB).

100  $\mu\text{g/ml}$  in the extract group ( $69.09 \pm 5.33\%$ ) when compared to the AgNPs-W ( $54.28 \pm 1.48\%$ ,  $p \leq 0.005^{**}$ ) and AgNP-M ( $54.83 \pm 2.53\%$ ,  $p \leq 0.006^{**}$ ); no differences were observed between AgNPs groups ( $p \leq 0.979$ ). No statistical significances were observed in the other concentrations (Figure 4(c), supplementary table 5).

**3.5. AgNPs Reduce Macrophage Cell Viability but Not in Fibroblast.** To evaluate the effect of AgNPs in nontumor cells, we chose human neonatal fibroblasts (HDFn cell line) and murine macrophages (RAW 264.7 cell line) and immune cell effectors. First, we found no differences between the groups at 100  $\mu\text{g/ml}$  (extract:  $50.72 \pm 29.78\%$  vs AgNP-W:  $45.90 \pm 21.70\%$ ,  $p \leq 0.966$ ; vs AgNP-M:  $42.97 \pm 18.38\%$ ,  $p \leq 0.987$ ) and 50  $\mu\text{g/ml}$  (extract:  $96.18 \pm 26.41\%$  vs AgNP-W:  $49.78 \pm 17.56\%$ ,  $p \leq 0.091$ ; vs AgNP-M:  $44.85 \pm 21.12\%$ ,  $p \leq 0.065$ ). Then, we observe differences at 25  $\mu\text{g/ml}$  in the extract group ( $123.75 \pm 10.92\%$ ) vs the AgNP-W ( $53.45 \pm 23.92\%$ ,  $p \leq 0.023^{*}$ ) and AgNP-M ( $50.29 \pm 30.75\%$ ,  $p \leq 0.019^{*}$ ) groups. Those differences persist at 12.5  $\mu\text{g/ml}$  (extract:  $119.22 \pm 7.80\%$  vs. AgNP-W:  $80.12 \pm 18.39\%$ ,  $p \leq 0.017^{*}$ ; vs. AgNP-M:  $83.93 \pm 6.62\%$ ,  $p \leq 0.027^{*}$ ). No statistical differences were observed at other

concentrations (Figure 4(d), supplementary table 6). In contrast to macrophages, fibroblasts only display a reduction in cell viability at 100  $\mu\text{g/ml}$  between the extract group ( $54.63 \pm 9.90\%$ ) vs. the AgNPs-W group ( $32.49 \pm 4.15\%$ ,  $p \leq 0.037^{*}$ ) and no differences between the extract and AgNP-M ( $45.10 \pm 9.28\%$ ,  $p \leq 0.387$ ) were observed. See Figure 4(e) and supplementary Table 7.

## 4. Discussion

In the present study, we synthesized AgNPs from the peel of *A. muricata* and, as previously reported, obtained spheroid nanoparticles with optical properties similar to those reported by Gonzalez-Pedroza and colleagues [2]. In the UV/Vis analysis, we obtained a band ranging from 400 to 450 nm in the three AgNPs' solutions, which indicated the presence of AgNPs in the solutions evaluated [18]. The peak observed at the 440 nm emission peak in the cell culture medium solution of both AgNPs possibly indicates some interaction due to the components of each cell culture medium. To determine the size and morphology of the AgNPs, we conducted TEM analysis, which revealed that the



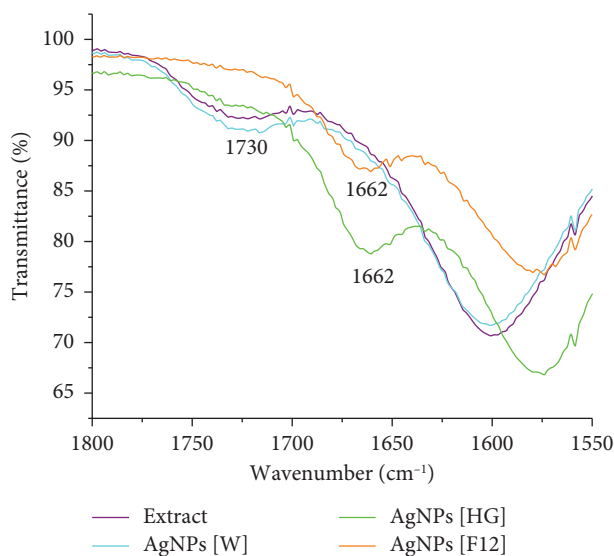


FIGURE 3: AgNPs functional groups' characterization. FTIR spectra for the four solutions evaluated, the vibrational bands represent the lactone in the acetogenins. Extract (purple), AgNPs in water-extract (AgNPs [W], light blue), AgNPs in the HG cell culture medium (AgNPs [HG], green), and AgNPs in the F12 cell culture medium (AgNPs [F12], orange).

cell culture medium did not alter the morphology of the AgNPs or size of the nanoparticles. Furthermore, the FTIR analysis shows a signal at  $1730\text{ cm}^{-1}$  corresponding to the conjugated C=O group present in the aqueous extract, which we associate with an  $\alpha$ ,  $\beta$ -unsaturated  $\gamma$ -lactone that distinguishes the vast majority of acetogenins. Likewise, the same signal is observed but more intense in the AgNP-W solutions. In the AgNP-M (HG and F12) solutions, certain regions are identified with displacements of this characteristic group up to  $1662\text{ cm}^{-1}$ . This may be due to the compounds present in the culture medium and their interaction.

In previous reports, the antitumor effect of AgNPs from *A. muricata* peel has been demonstrated in melanoma, colon, and breast cancer cell lines [2]. In this study, we presented the effect of AgNPs on the viability of brain tumor cell lines. Additionally, we compared the effect of AgNPs in cell culture media to reduce the cytotoxic effects on nontumor cells. First, we observe that AgNPs in water and the cell culture medium in Daoy medulloblastoma cells show a lower viability at 100 and  $50\text{ }\mu\text{g/ml}$  compared to the extract group. In contrast, in the D341 Med medulloblastoma cell line, only the AgNPs in the cell culture medium significantly reduce the cell viability at 100 and  $50\text{ }\mu\text{g/ml}$  compared to the extract group. Conversely, neuroblastoma cells show reduced viability at  $100\text{ }\mu\text{g/ml}$  of AgNPs in water and the cell culture medium in contrast to the extract group.

To date, it is well known that soursop contains bioactive compounds like alkaloids, cyclopeptides, phenolics, essential oils, flavonol triglycosides, megastigmanes, and annonaceous acetogenins [4]. And, as mentioned above, the *A. muricata* acetogenins are the responsible bioactive compounds of the antitumor effect of soursop [19]. The

antitumor mechanism of acetogenins includes inhibiting the ATP production in the mitochondria by repressing the complex I [20, 21] and NADH oxidase in the membrane [22–25]. Respiratory complex I, alongside the other electron transport chain complexes, is necessary for cell function and life and is the primary source of ATP [26, 27]. In addition, medulloblastoma cells overexpress respiratory complex I [28]. Thus, acetogenins appear to affect the tumor cell metabolic pathways since medulloblastoma, depending on the subgroup, display alterations in their metabolic pathways [29, 30]. Since ATP production in the Daoy cell line is elevated [31], this suggests that AgNPs capped with acetogenins may impair Daoy cell metabolism. Probably, this elevated ATP production is also present in the D341 Med cell line, but this mechanism has not yet been demonstrated. Both cell lines (Daoy and D341 Med) decrease their viability after soursop AgNPs administration, at least in the two highest concentrations, while central nervous system (CNS) neuroblastoma cells (CHP-2012) decrease only at  $100\text{ }\mu\text{g/ml}$ , thus probably because neuroblastoma could express in lesser respiratory complex I and other ATP-dependent proteins. Of note, neuroblastoma is classified as a grade 2–4 tumor (classification still debatable), and metabolic machinery in those tumors is less prominent.

On the other hand, the metal NPs from soursop (zinc, copper, and silver) have been studied for antitumor effects [32–34]. AgNPs promote apoptosis through overexpression of caspase-9 and downregulation of CXCL1 in HeLa and prostate adenocarcinoma cells [35]. Another study showed that AgNPs from soursop peel induce apoptosis and autophagy in AMJ13 and THP-1 cells by overexpression of p53, IL-1 $\beta$ , and reducing the activation of NLRP3 inflammasome [36]. Also, overexpression of p21, p53, BAX, caspase 8, 9, and 3, increased levels of reactive oxygen species (ROS), and downregulation of BCL-2 and cyclins E, B, and D in the A549 cell line are observed after soursop AgNPs' administration [37]. These studies highlight the diverse pathways in which soursop AgNPs show cytotoxic effects over tumor cells.

In perspective, as acetogenins inhibit the ATP production, in a scenario where medulloblastoma cells can develop multidrug resistance, soursop AgNPs may reduce the P-glycoproteins' (Pgp) function [38, 39], an ATP-binding cassette (ABC) transporter, which is expressed in Daoy (SHH medulloblastoma subgroup) and D341 Med (Group 3 medulloblastoma) cell lines [40, 41], by decreasing the ATP production in the tumor cell, highlighting a promising role of AgNPs in chemosensitivity. Therefore, soursop AgNPs could be a promising tool for medulloblastoma treatment.

To evaluate the AgNPs in nontumor cells, we tested the AgNPs in macrophages (RAW 264.7) and fibroblasts (HDFn). Macrophages were highly susceptible to the AgNPs in water and the cell culture medium and peel extract at 100 and  $50\text{ }\mu\text{g/ml}$ . This effect persists at 25 and  $12.5\text{ }\mu\text{g/ml}$  for the AgNPs groups. Macrophages are phagocytic cells, which are probably phagocyte AgNPs that promote a high intracellular concentration, triggering cell death by promoting the release of proinflammatory cytokines and ROS [42, 43]. This issue

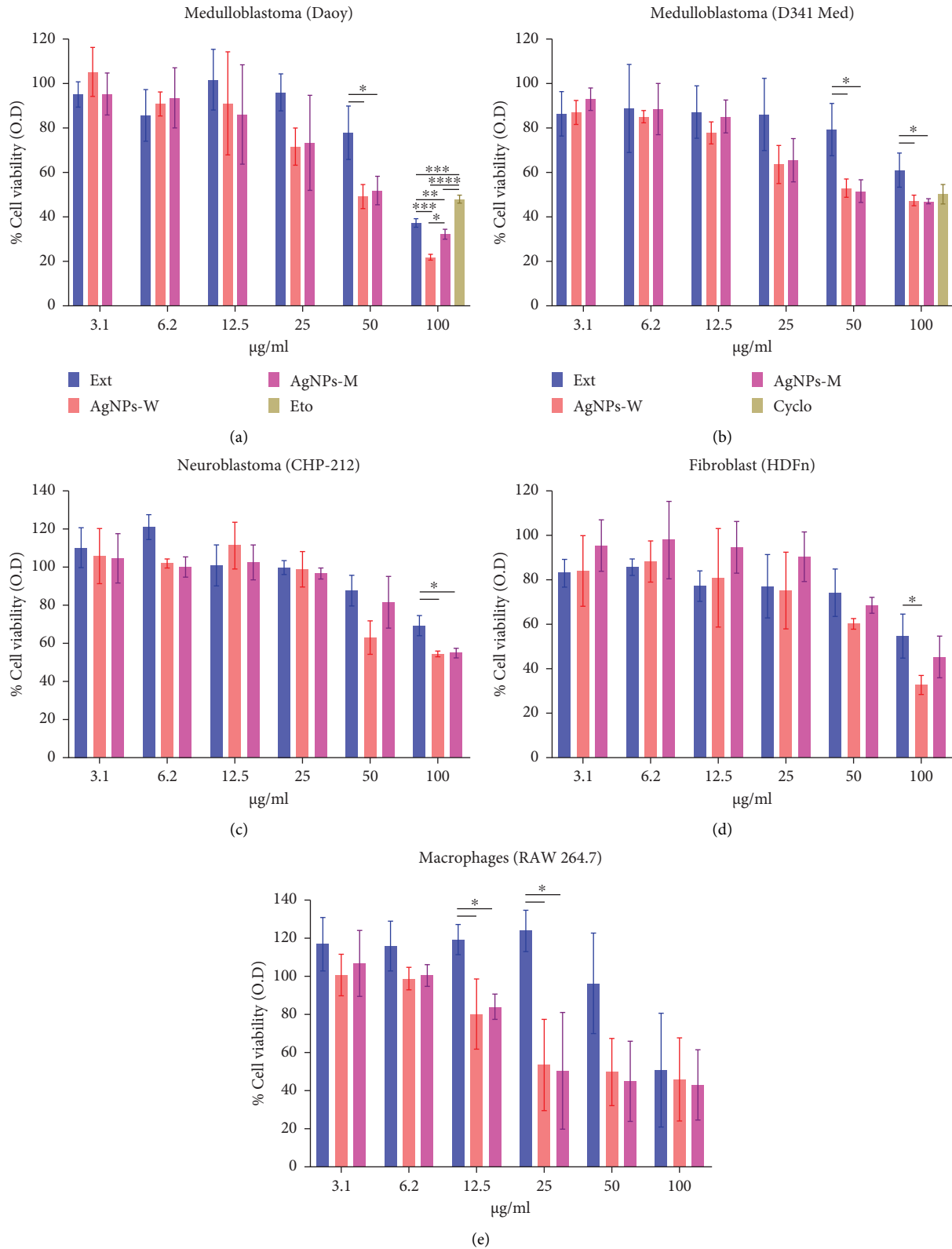


FIGURE 4: Cell viability after AgNPs' administration. Medulloblastoma cell lines Daoy (a) and D341 Med (b), neuroblastoma CHP-212 (c), macrophages RAW 264.7 (d), and HDFn fibroblasts (e). All procedures were processed by triplicates;  $n = 3$  per group. Data are expressed as the mean  $\pm$  SD. One-way ANOVA, *post-hoc* Tukey HSD test. \*  $p = \leq 0.05$ .

could be overcome by tailoring the AgNPs with some molecules that help avoid the macrophage's recognition, activation, and subsequent phagocytosis [44]. In HDFn cells, we observed that AgNPs reduce the fibroblast viability only at the highest concentration (100  $\mu\text{g/ml}$ ), with the AgNPs in water displaying a more significant cytotoxic effect compared to the extract and group. Here, we report for the first time the effect of soursop peel-derived AgNPs on the viability of medulloblastoma and neuroblastoma cells.

## 5. Limitations of the Study

In our study, we synthesized and characterized AgNPs based on *A. muricata* peel aqueous extracts. The use of additional techniques could be useful to characterize the AgNPs and the extract, which in turn can give us valuable information about their composition. On the other hand, the MTT assay foundation lies in detecting viable cells by their metabolic activity. In this regard, techniques that help elucidate the specific cellular processes involved in response to AgNPs are necessary. Nevertheless, as a first step, MTT is a valuable assay for observing the effect of AgNPs and other materials with potential clinical relevance.

## 6. Conclusion

In compendium, we observed that soursop AgNPs reduce tumor cell line viability, with a better effect over medulloblastoma cells. Also, AgNPs have a limited impact on fibroblasts, whereas macrophages appear perturbed at the highest concentrations. AgNPs obtained from *A. muricata* could represent a useful tool for brain tumor treatment. However, studies to elucidate the cytotoxic mechanism are necessary.

## Data Availability

All the datasets generated during and/or analyzed during the current study are available from the corresponding author upon request.

## Conflicts of Interest

The authors declare that they have no conflicts of interest.

## Authors' Contributions

ELD conducted conceptualization, methodology, formal analysis, investigation, and writing the original draft. RCM conducted methodology, formal analysis, and investigation. MGGP conducted methodology, formal analysis, and investigation. OGP conducted visualization, supervision, and editing. RAML conducted visualization, supervision, writing, reviewing, and editing. JJAF conducted visualization, supervision, writing, reviewing, and editing, and project administration and collected resources.

## Acknowledgments

CONAHCyT. CVU: 736004.

## Supplementary Materials

Supplementary table 1: Daoy cell line statistics. Supplementary table 2: Daoy cell line statistics, etoposide. Supplementary table 3: D341 Med cell line statistics. Supplementary table 4: D341 Med cell line statistics, Cyclophosphamide. Supplementary table 5: CHP-212 cell line statistics. Supplementary table 6: raw 264.7 cell line statistics. Supplementary table 7: HDFn cell line statistics. (*Supplementary Materials*)

## References

- [1] L. Wei, J. Lu, H. Xu, A. Patel, Z. S. Chen, and G. Chen, "Silver nanoparticles: Synthesis, properties, and therapeutic applications," *Drug Discovery Today*, vol. 20, no. 5, pp. 595–601, 2015.
- [2] M. G. González-Pedroza, L. Argueta-Figueroa, R. García-Contreras et al., "Silver nanoparticles from *Annona muricata* peel and leaf extracts as a potential potent, biocompatible and low cost antitumor tool," *Nanomaterials*, vol. 11, no. 5, p. 1273, 2021.
- [3] R. R. Miranda, I. Sampaio, and V. Zucolotto, "Exploring silver nanoparticles for cancer therapy and diagnosis," *Colloids and Surfaces B: Biointerfaces*, vol. 210, Article ID 112254, 2022.
- [4] N. Badrie and A. G. Schauss, "Soursop (*Annona muricata* L.): composition, nutritional value, medicinal uses, and toxicology," in *Bioactive Foods in Promoting Health*, pp. 621–643, Academic Press, Cambridge, MA, USA, 2010.
- [5] S. Z. Moghadamtousi, M. Fadaeinasab, S. Nikzad, G. Mohan, H. M. Ali, and H. A. Kadir, "*Annona muricata* (Annonaceae): A review of its traditional uses, isolated acetogenins and biological activities," *International Journal of Molecular Sciences*, vol. 16, no. 7, pp. 15625–15658, 2015.
- [6] M. P. Torres, S. Rachagani, V. Purohit et al., "Graviola: A novel promising natural-derived drug that inhibits tumorigenicity and metastasis of pancreatic cancer cells in vitro and in vivo through altering cell metabolism," *Cancer letters*, vol. 323, no. 1, pp. 29–40, 2012.
- [7] S. Z. Moghadamtousi, H. A. Kadir, M. Paydar, E. Rouhollahi, and H. Karimian, "*Annona muricata* leaves induced apoptosis in A549 cells through mitochondrial-mediated pathway and involvement of NF- $\kappa$ B," *BMC Complementary and Alternative Medicine*, vol. 14, no. 1, pp. 299–313, 2014.
- [8] D. Daddiouaissa, A. Amid, N. A. Kabbashi, F. A. Fuad, A. M. Elnour, and M. A. Epany, "Antiproliferative activity of ionic liquid-graviola fruit extract against human breast cancer (MCF-7) cell lines using flow cytometry techniques," *Journal of Ethnopharmacology*, vol. 236, pp. 466–473, 2019.
- [9] K. Foster, O. Oyenih, S. Rademan et al., "Selective cytotoxic and anti-metastatic activity in DU-145 prostate cancer cells induced by *Annona muricata* L. bark extract and phytochemical, annonacin," *BMC Complementary Medicine and Therapies*, vol. 20, pp. 375–415, 2020.
- [10] F. Qorina, A. Arsianti, Q. Fithrotunnisa, N. Tejaputri, N. N. Azizah, and R. Putrianiingsih, "Cytotoxicity of soursop leaves (*Annona muricata*) against cervical HeLa cancer cells," *Pharmacognosy Journal*, vol. 12, no. 1, pp. 20–24, 2020.
- [11] V. S. Shaniba, A. A. Aziz, J. Joseph, P. R. Jayasree, and P. R. Manish Kumar, "Synthesis, characterization and evaluation of antioxidant and cytotoxic potential of *Annona muricata* root extract-derived biogenic silver nanoparticles," *Journal of Cluster Science*, vol. 33, no. 2, pp. 467–483, 2022.

- [12] D. N. Louis, P. Wesseling, K. Aldape et al., “cIMPACT-NOW update 6: new entity and diagnostic principle recommendations of the cIMPACT-Utrecht meeting on future CNS tumor classification and grading,” *Brain Pathology*, vol. 30, 2020.
- [13] J. A. Cotter and C. Hawkins, “Medulloblastoma: WHO 2021 and beyond,” *Pediatric and Developmental Pathology*, vol. 25, no. 1, pp. 23–33, 2022.
- [14] A. Tietze, K. Mankad, M. H. Lequin et al., “Imaging characteristics of CNS neuroblastoma-FOXR2: A retrospective and multi-institutional description of 25 cases,” *American Journal of Neuroradiology*, vol. 43, no. 10, pp. 1476–1480, 2022.
- [15] D. N. Louis, A. Perry, P. Wesseling et al., “The 2021 WHO classification of tumors of the central nervous system: A summary,” *Neuro-Oncology*, vol. 23, no. 8, pp. 1231–1251, 2021.
- [16] D. N. Louis, H. Ohgaki, O. D. Wiestler et al., “The 2007 WHO classification of tumours of the central nervous system,” *Acta Neuropathologica*, vol. 114, no. 5, pp. 547–109, 2007.
- [17] T. Komori, “The 2021 WHO classification of tumors, 5th edition, central nervous system tumors: the 10 basic principles,” *Brain Tumor Pathology*, vol. 39, no. 2, pp. 47–50, 2022.
- [18] K. F. Hasan, L. Xiaoyi, Z. Shaoqin et al., “Functional silver nanoparticles synthesis from sustainable point of view: 2000 to 2023—A review on game changing materials,” *Heliyon*, vol. 8, no. 12, Article ID e12322, 2022.
- [19] S. Bernitsa, R. Dayan, A. Stephanou, I. D. Tzvetanova, and I. S. Patrikios, “Natural biomolecules and derivatives as anticancer immunomodulatory agents,” *Frontiers in Immunology*, vol. 13, Article ID 1070367, 2022.
- [20] M. Londershausen, W. Leicht, F. Lieb, H. Moeschler, and H. Weiss, “Molecular mode of action of annonins,” *Pesticide Science*, vol. 33, no. 4, pp. 427–438, 1991.
- [21] M. A. Lewis, J. T. Arnason, B. J. R. Philogene, J. K. Rupprecht, and J. L. McLaughlin, “Inhibition of respiration at site I by asimicin, an insecticidal acetogenin of the pawpaw, *Asimina triloba* (Annonaceae),” *Pesticide Biochemistry and Physiology*, vol. 45, no. 1, pp. 15–23, 1993.
- [22] K. I. Ahammadsahib, R. M. Hollingworth, J. P. McGovren, Y. H. Hui, and J. L. McLaughlin, “Mode of action of bullatacin: A potent antitumor and pesticidal annonaceous acetogenin,” *Life Sciences*, vol. 53, no. 14, pp. 1113–1120, 1993.
- [23] D. James Morr , R. de Cabo, C. Farley, N. H. Oberlies, and J. L. McLaughlin, “Mode of action of bullatacin, a potent antitumor acetogenin: Inhibition of NADH oxidase activity of HeLa and HL-60, but not liver, plasma membranes,” *Life Sciences*, vol. 56, no. 5, pp. 343–348, 1994.
- [24] M. Degli Esposti, A. Ghelli, M. Ratta, D. Cortes, and E. Estornell, “Natural substances (acetogenins) from the family Annonaceae are powerful inhibitors of mitochondrial NADH dehydrogenase (Complex I),” *Biochemical Journal*, vol. 301, no. 1, pp. 161–167, 1994.
- [25] N. H. Oberlies, C. J. Chang, and J. L. McLaughlin, “Structure-Activity relationships of diverse annonaceous acetogenins against multidrug resistant human mammary adenocarcinoma (MCF-7/Adr) Cells,” *Journal of Medicinal Chemistry*, vol. 40, no. 13, pp. 2102–2106, 1997.
- [26] L. A. Sazanov, “A giant molecular proton pump: Structure and mechanism of respiratory complex I,” *Nature Reviews Molecular Cell Biology*, vol. 16, no. 6, pp. 375–388, 2015.
- [27] K. Parey, C. Wirth, J. Vonck, and V. Zickermann, “Respiratory complex I—structure, mechanism and evolution,” *Current Opinion in Structural Biology*, vol. 63, pp. 1–9, 2020.
- [28] L. K. Sharma, J. Lu, and Y. Bai, “Mitochondrial respiratory complex I: Structure, function and implication in human diseases,” *Current Medicinal Chemistry*, vol. 16, no. 10, pp. 1266–1277, 2009.
- [29] P. A. Northcott, I. Buchhalter, A. S. Morrissy et al., “The whole-genome landscape of medulloblastoma subtypes,” *Nature*, vol. 547, no. 7663, pp. 311–317, 2017.
- [30] A. K. Park, J. Y. Lee, H. Cheong et al., “Subgroup-specific prognostic signaling and metabolic pathways in pediatric medulloblastoma,” *BMC Cancer*, vol. 19, no. 1, pp. 571–615, 2019.
- [31] A. R. Cappellari, L. Rockenbach, F. Dietrich et al., “Characterization of ectonucleotidases in human medulloblastoma cell lines: Ecto-5’ NT/CD73 in metastasis as potential prognostic factor,” *PLoS One*, vol. 7, no. 10, Article ID e47468, 2012.
- [32] R. I. Mahmood, A. A. Kadhim, S. Ibraheem et al., “Biosynthesis of copper oxide nanoparticles mediated *Annona muricata* as cytotoxic and apoptosis inducer factor in breast cancer cell lines,” *Scientific Reports*, vol. 12, no. 1, Article ID 16165, 2022.
- [33] H. Asadevi, P. Prasannakumaran Nair Chandrika Kumari, R. Padmavati Amma, S. A. Khadar, S. Charivumvasathu Sasi, and R. Raghunandan, “ZnO@ MOF-5 as a fluorescence “Turn-Off” sensor for ultrasensitive detection as well as probing of Copper (II) ions,” *ACS Omega*, vol. 7, no. 15, pp. 13031–13041, 2022.
- [34] P. S. Vindhya, S. Suresh, R. Kunjikannan, and V. T. Kavitha, “Antimicrobial, antioxidant, cytotoxicity and photocatalytic performance of Co doped ZnO nanoparticles biosynthesized using *Annona muricata* leaf extract,” *Journal of Environmental Health Science and Engineering*, vol. 21, pp. 167–185, 2023.
- [35] Y. Gavamukulya, E. N. Maina, H. A. El-Shemy et al., “*Annona muricata* silver nanoparticles exhibit strong anticancer activities against cervical and prostate adenocarcinomas through regulation of CASP9 and the CXCL1/CXCR2 genes axis,” *Tumor Biology*, vol. 43, no. 1, pp. 37–55, 2021.
- [36] M. S. Jabir, Y. M. Saleh, G. M. Sulaiman et al., “Green synthesis of silver nanoparticles using *Annona muricata* extract as an inducer of apoptosis in cancer cells and inhibitor for NLRP3 inflammasome via enhanced autophagy,” *Nanomaterials*, vol. 11, no. 2, p. 384, 2021.
- [37] S. Meenakshisundaram, V. Krishnamoorthy, Y. Jagadeesan, R. Vilwanathan, and A. Balaiah, “*Annona muricata* assisted biogenic synthesis of silver nanoparticles regulates cell cycle arrest in NSCLC cell lines,” *Bioorganic Chemistry*, vol. 95, Article ID 103451, 2020.
- [38] D. M. Tishler and C. Raffel, “Development of multidrug resistance in a primitive neuroectodermal tumor cell line,” *Journal of Neurosurgery*, vol. 76, no. 3, pp. 502–506, 1992.
- [39] M. J. Lee, B. A. Hatton, E. H. Villavicencio et al., “Hedgehog pathway inhibitor saridegib (IPI-926) increases lifespan in a mouse medulloblastoma model,” *Proceedings of the National Academy of Sciences*, vol. 109, no. 20, pp. 7859–7864, 2012.
- [40] D. P. Ivanov, B. Coyle, D. A. Walker, and A. M. Grabowska, “In vitro models of medulloblastoma: choosing the right tool for the job,” *Journal of Biotechnology*, vol. 236, pp. 10–25, 2016.
- [41] E. Martell, H. Kuzmychova, E. Kaul et al., “Metabolism-based targeting of MYC via MPC-SOD2 axis-mediated oxidation promotes cellular differentiation in group 3 medulloblastoma,” *Nature Communications*, vol. 14, no. 1, p. 2502, 2023.



- [42] R. Arruda da Silva Sanfelice, T. F. Silva, F. Tomiotto-Pellissier et al., “Biogenic silver nanoparticles reduce *Toxoplasma gondii* infection and proliferation in RAW 264.7 macrophages by inducing tumor necrosis factor-alpha and reactive oxygen species production in the cells,” *Microbes and Infection*, vol. 24, no. 5, Article ID 104971, 2022.
- [43] A. Sousa, A. T. Rufino, R. Fernandes et al., “Silver nanoparticles exert toxic effects in human monocytes and macrophages associated with the disruption of  $\Delta\psi_m$  and release of pro-inflammatory cytokines,” *Archives of Toxicology*, vol. 97, no. 2, pp. 405–420, 2023.
- [44] Y. Xia, L. Rao, H. Yao, Z. Wang, P. Ning, and X. Chen, “Engineering macrophages for cancer immunotherapy and drug delivery,” *Advanced Materials*, vol. 32, no. 40, Article ID e2002054, 2020.